JOURNAL OF MOLECULAR SPECTROSCOPY 66, 133–149 (1977)

The Infrared Spectrum of C_3O_2

The Interaction between ν_7 and the ν_2 and ν_4 Vibrations

C. W. PETERS

Physics Department, University of Michigan, Ann Arbor, Michigan 48109

AND

W. H. WEBER AND P. D. MAKER

Physics Department, Research Staff, Ford Motor Company, Dearborn, Michigan 48121

The $3\nu^1_7$, $3\nu^3_7$, and $4\nu^0_7$ hot bands of the ν_4 fundamental of C_3O_2 in the 1580 cm^{-1} region were analyzed from tunable diode laser spectra and the ground state to $\nu_4 + 2\nu^0_7$ band at 1644 cm^{-1} from Fourier transform spectra (FTS). The molecular constants for all of the v_4 1 ← 0 bands as well as the intensity of the $\nu_4 + 2\nu^0_7$ sum band relative to the ν_4 fundamental were in agreement with the predictions of the model of Weber and Ford. FTS spectra at 0.05 cm^{-1} resolution were obtained of the sum and difference bands of ν_2 with ν_7 in the 750–900 cm^{-1} region. Sharp Q branches occur for each ν_7 state in the sum bands, but only a number of R-branch bandheads and no recognizable Q branches in the difference bands. Assignments of the sum band Q branches through $v_7 = 6$ were made and molecular constants were determined for the $\nu_2 + \nu^1_7 \leftarrow 0$ transition at 819.7 cm^{-1}. The ν_7 potential function in the $v_2 = 1$ state was found to have a 1.2 cm^{-1} barrier with a minimum at $\alpha = 4.9°$, where 2α is the angular deviation from linearity. The Q-branch positions predicted from the calculated energy levels fit those observed within several cm^{-1}.

I. INTRODUCTION

Measurements with tunable diode lasers in the region of absorption by the ν_4 fundamental of C_3O_2 between 1565 and 1600 cm^{-1} were recently reported (*1*). Some six overlapping bands having P- and R-branch structures indicative of a linear molecule were analyzed. The ν_4 fundamental was identified as being centered at 1587.39 cm^{-1}. The five other bands were labeled as "hot bands" involving the excited states of the ν_7 bending mode: $1\nu^1_7$, $2\nu^0_7$, and $2\nu^2_7$. The extremely low frequency of the ν_7 vibration, about 18–19 cm^{-1}, results in an appreciable population in many of the excited states of ν_7. Our early attempts to identify series of lines for higher excited states of ν_7 were fruitless. There were a multitude of weaker lines, but we could not recognize any complete P- and R-branch series.

More recently, vibration–rotation energy levels for the ν_7 mode have been given by Weber and Ford (*2*) assuming a simple model of C_3O_2: rigid O–C–C bonds fixed at 180° and an anharmonic potential for the ν_7 vibration. The parameters in the model were fixed by three quantities determined from experiments: the rotational constant B in

ISSN 0022-2852

the ground state, B in the $2\nu^0_7$ state, and the separation of the ground and $2\nu^0_7$ states. In a similar way they evaluated the vibration–rotation energy levels when ν_4 was simultaneously excited; the fixed quantities being B in the ν_4 state, B in the $\nu_4 + 2\nu^0_7$ state, and the energy separation of the ν_4 and $\nu_4 + 2\nu^0_7$ states. From these energy level values the P- and R-line positions could be predicted for any ν_7 "hot band" in the ν_4 transitions. Using these values as a guide we have been able to identify and analyze the $3\nu^1_7$, $3\nu^3_7$, and $4\nu^0_7$ hot bands, in the spectra of the ν_4 fundamental taken previously.

Calculations on a similar model have been made by Duckett, Mills, and Robiette (*3*). These give nearly the same results for the ν_7 energy levels and B values as the model of Weber and Ford. However, they do not lead to values for the centrifugal distortion constants.

From additional spectra taken with the Fourier transform spectrometer used in Ref. (*1*), we have concluded that most of the absorption in the 1660 cm^{-1} region can be attributed to transitions of the type $\Delta v_4 = 1$, $\Delta v_7 = 2$, $\Delta l = 0$. The lowest lying of these is the ground state to $\nu_4 + 2\nu^0_7$ transition, centered at 1644.14 cm^{-1}. An analysis of this band coupled with the measurement of the $2\nu^0_7$ energy by Mantz *et al.* (*4*) indicates that the J assignments previously reported (*1*) for the $\nu_4 + 2\nu^0_7 \leftarrow 2\nu^0_7$ transitions should all be shifted to higher frequency by one line position. With this correction the $2\nu^0_7$ energy is found to be 60.71 ± 0.05 cm^{-1}, in agreement with other results (*4*, *5*).

The Fourier transform spectrometer has also been used to examine the weak combination and difference bands involving ν_7 and the Raman-active ν_2 fundamental at 786.1 cm^{-1}. Fine structure in this region of the infrared spectrum was first reported by Miller and Fateley (*6*), but it was only recently identified with the $\nu_2 \pm \nu_7$ combination bands (*3*). Sharp Q branches associated with $\Delta v_7 = +1$ are observed in the sum band, while R-branch bandheads associated with $\Delta v_7 = -1$ are observed in the difference band.

II. EXPERIMENTAL DETAILS

The same Doppler-limited, diode laser spectra reported in Ref. (*1*) were used in obtaining the data presented here for the ν_4 fundamental.

The Fourier transform spectrometer system consisted of an Eocom Model 7001 rapid scan Michelson interferometer controlled by a He–Ne laser with a KBr beam splitter, a liquid N_2 cooled HgCdTe detector from Santa Barbara Research Center, an Analogic 15 bit analog to digital converter and a PDP 11/40 computer with dual RK05 disk drives, 24K core memory, scope display and x–y plotter. Electronics, interfacing, optical layout, and computer softwave were in-house efforts. The optics were enclosed in a hermetically sealed lucite box. The ultradry tank nitrogen air bearing supply also purged this box, reducing peak absorption in the background spectrum due to ambient water vapor and carbon dioxide to less than 50%. Producing the spectra began with the co-addition of 64 consecutive one-sided interferograms, each consisting of about 117 000 data points corresponding to the maximum instrumental retardation of 15 cm. This took about 5 min. The amplifier used was gain-switched to reduce digitization noise. It also incorporated a nonlinear stage to compensate for optical saturation of the detector response (*7*). No mathematical apodization was applied. A fast Fourier transform was then performed following the algorithm of Bergland (*8*). This used only half the space

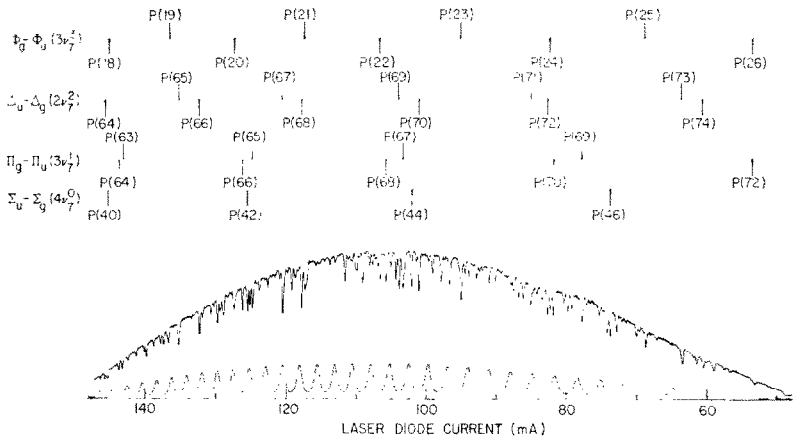

FIG. 1. A 1.1 cm^{-1} scan of the ν_4 absorption of C_3O_2 about 1566 cm^{-1}, obtained with a thin-film PbTe diode laser. The sample pressure was 0.1 Torr, the path length 3.2 m. The fringed curve is the channel spectrum of a 3.7879 cm polycrystalline Ge etalon (free spectral range 0.032770 cm^{-1}) recorded simultaneously with the C_3O_2 spectrum using a double beam technique. The rotational assignments and the ν_7 states are indicated.

and half the computation required for a complex input data set. The resultant data set was corrected for optical phase variations (*9*) using linear interpolation of a 64 point phase function determined from an interferogram recorded with no sample present. This function varied no more than $\pm 60°$ over the whole instrumental spectral range. The final spectrum digitized at 0.015 cm^{-1} intervals from zero to 3950 cm^{-1} (a total of $\sim$250 000 points) emerged some 30 min after processing began. Usable signal extended from 600 to 3800 cm^{-1}, with the signal to rms noise ratio reaching 1000:1 in the 800 to 2000 cm^{-1} region. The spectra were plotted with a linear decimal-absorbance abscissa, obtained by taking the logarithmic ratio of spectra without and with the sample present, after each had been decreased by a room-temperature-source background spectrum. This latter correction was necessary to obtain the true absorbance because, due to imperfect optical elements, some modulated radiation which had not passed through the absorption cell fell on the detector. No further interpolation was used, the traces shown being point by point line plots of the so derived data. At low pressures of the sample, the instrumental response function could be observed. It was found to closely approximate the expected $\sin x/x$, and had a half-height width of 0.039 cm^{-1}. For the sample used (0.2 Torr with ultrapure argon in a 40 pass White cell with 40 m path length) the lines broadened to about 0.05 cm^{-1} and the secondary artificial maxima were greatly reduced. The spectra are believed to be accurate to $\pm 10\%$ in absorbance. Line positions could be read directly, with no external calibration, to ± 0.02 cm^{-1}. With an expanded plot and calibration by known absorption lines, the accuracy was improved to ± 0.005 cm^{-1}.

III. HOT BANDS OF ν_4

Using as a guide the values calculated by Weber and Ford (*2*) for the band centers and line spacings for the hot bands of ν_4, we were able to identify transitions involving the excited states $3\nu^1_7$, $3\nu^3_7$, and $4\nu^0_7$ in the diode laser spectra previously taken. Figure 1

TABLE I. Observed frequencies (vac. cm^{-1}) of the $\nu_4 + 3\nu_7^{1e} \leftarrow 3\nu_7^{1e}$ transitions. The rms error of the fit using the molecular constants in Tables VI and VII is ± 0.0028 cm^{-1} for 55 lines.

J	R(J) OBS.	O-C x 10^3	P(J) OBS.	O-C x 10^3
5			1575.2360	4.1
7	1577.2324	1.9		
9	77.5431	1.4	74.6321	6.5
11	77.8548	0.9		
13	78.1679	0.8		
15	78.4793	-2.0	73.7273	3.7
17	78.7971	0.7	73.4228	-2.1
19	79.1082	-4.3	73.1263	-0.9
21	79.4268	-2.7	72.8314	0.9
23	79.7421	-5.4	72.5336	-1.2
25			72.2374	-2.7
27	80.3822	-4.0	71.9428	-3.5
29	80.7000	-6.9		
37	81.9969	-1.5		
39	82.3235	0.2		
41	82.6495	0.6		
43	82.9759	0.6		
45	83.3055	3.1		
47	83.6355	5.4	69.0615	2.8
49	83.9584	-0.1	68.7811	6.7
51	84.2874	-0.0	68.4926	1.7
53	84.6176	0.7	68.2077	-0.4
55	84.9486	1.8	67.9260	0.1
57	85.2808	3.6	67.6461	1.9
59	85.6085	0.5	67.3646	1.4
61	85.9376	-1.4	67.0823	-0.3
63	86.2705	0.2	66.8012	-1.2
65	86.6011	-0.7	66.5216	-1.0
67	86.9307	-2.6	66.2428	-0.2
69	87.2613	-3.6	65.9625	-1.3
71	87.5924	-3.9		
73	87.9244	-3.2		
75	88.2569	-1.6		
77	88.5886	-0.5		
79	88.9207	1.6		
81	89.2541	5.6		

shows a 1.1 cm^{-1} scan near 1566 cm^{-1} in the lowest frequency region we studied. The fringed curve, used for calibration, is obtained simultaneously with the C_3O_2 spectrum by passing part of the beam through a Ge etalon. Our assignments for the P branches of the $2\nu^2_7$, $3\nu^{1,3}_7$, and $4\nu^0_7$ hot bands of the ν_4 $1 \leftarrow 0$ transitions are shown at the top of the figure. The assignment of the $3\nu^1_7$ series confirms the tentative assignments of the R branches of these series in Fig. 5 of Ref. (*1*).

Tables I–V gave the observed line positions for the new bands which we have analyzed along with the observed-minus-calculated errors. The lines of each band (the even and odd J's being treated as separate series) were fit to the formula

$$\nu = \nu_0 + (B' + B'')m + (B' - B'')m^2 - 2(D' + D'')m^3 - (D' - D'')m^4 + 3(H' + H'')m^5 + (H' - H'')m^6, \quad (1)$$

where $m = -J$ for the P branch and $m = J + 1$ for the R branch. Note that all of the explicit l dependence is included in ν_0, the band origin. This is the same procedure followed by Weber and Ford (*2*). Differences in ν_0 between the even and odd J series for the same v^l_7 state (which should be zero) reflect the reliability of the measurements and assignments. The bands were analyzed separately in this manner to ensure that their identifications were valid. This was of concern to us because of the gaps in our spectra and the fact that the many series were overlapping each other. The calculated

positions were obtained by first determining the molecular constants B'', D'', and H'' with a least squares fit to the lower level combination differences. These values were then constrained in a second least squares "polynomial in m" fit to all the measured lines, which yielded values for ν_0, ΔB, ΔD, and ΔH. In refining the least squares fits, data points which showed large deviations from the fitted curves were omitted and the fitting procedure was repeated until no remaining points deviated by more than about $2\frac{1}{2}$ standard deviations from their calculated values. Such rejected data points are not included in the tables. Upper state perturbations are known to occur in many C_3O_2 bands, and for this reason we feel the above fitting procedure is more reliable than the one we used previously, which varied all seven band parameters simultaneously. Since we were never able to observe lines close to the band origins (lines with J less than 10 were quite weak) several different choices for the J numbering of each band had to be tried, and the one giving the best fit and the most reasonable B'' and D'' values was selected. The theoretical predictions from Ref. (*2*) for the band origins and B values aided considerably in determining the "most reasonable" molecular constants.

Tables VI and VII summarize the results on the molecular constants for the lower and upper levels, respectively. For completeness we have also included the results from Ref. (*1*). These values differ slightly from those reported previously, since we have reanalyzed the data using the procedure described above, the corrected J assignments

TABLE II. Observed frequencies (vac. cm^{-1}) of the $\nu_4 + 3\nu_7^{1f} \leftarrow 3\nu_7^{1f}$ transitions. The rms error of the fit using the molecular constants in Tables VI and VII is ± 0.0028 cm^{-1} for 55 lines.

J	R(J) OBS.	O-C x 10^3	P(J) OBS.	O-C x 10^3
4	1576.7799	6.6	1575.3825	1.1
6			75.0802	4.1
8	77.4025	1.3		
10	77.7192	1.9		
12	78.0344	-0.5		
14	78.3486	-5.2	73.8743	4.9
16	78.6739	-0.2	73.5777	6.4
18			73.2724	-2.3
20			72.9821	2.6
22	79.6372	-6.1	72.6846	-1.1
24	79.9645	-4.6	72.3899	-3.4
26	80.2919	-4.2	72.0973	-5.1
28	80.6216	-2.9	71.8099	-2.9
36	81.9479	-2.4		
38	82.2834	-1.4		
40	82.6244	4.1		
42	82.9572	0.2		
44	83.2940	-0.7		
46	83.6356	2.2		
48	83.9791	6.1	68.9913	2.1
50	84.3123	-1.3	68.7150	1.5
52	84.6534	-1.6	68.4394	0.6
54	84.9955	-1.7	68.1649	-0.2
56	85.3400	-0.1	67.8925	0.2
58	85.6847	1.0	67.6222	1.7
60	86.0284	0.5	67.3496	0.1
62	86.3752	2.6	67.0791	-0.1
64	86.7202	2.5	66.8095	-0.2
66	87.0634	0.3	66.5414	0.7
68	87.4067	-2.2	66.2723	-0.0
70	87.7516	-3.1	66.0041	-0.2
72	88.0986	-2.0	65.7347	-2.0
74	88.4450	-1.4		
76	88.7922	0.1		
78	89.1406	3.2		

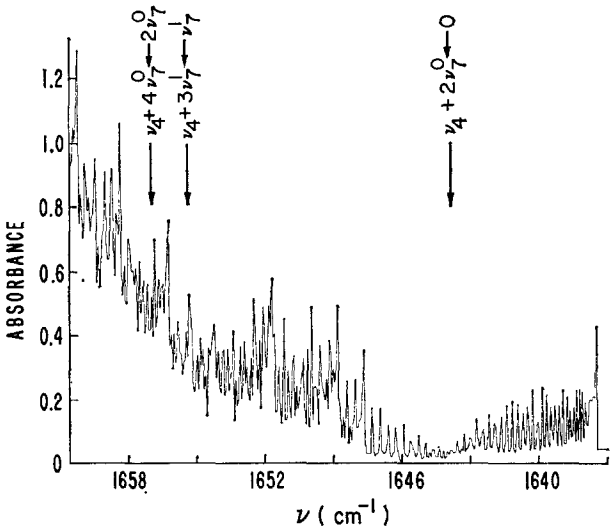

FIG. 2. Fourier transform spectrum of the low frequency side of the $\Delta v_4 = 1$, $\Delta v_7 = +2$, and $\Delta l = 0$ bands. The ground state band centered at 1644.14 cm^{-1} shows a bandhead in its P branch at 1637.5 cm^{-1}. Its higher R lines are overlapped by P lines of the hot bands. The predicted centers of the lowest frequency hot bands are indicated. C_3O_2 pressure 0.2 Torr, argon pressure 175 Torr, path length 40 m, and resolution 0.05 cm^{-1}.

in the $2\nu^0_7$ hot band have been included, and we have used improved measurements of the high-J, P-branch, Δ_u-Δ_g lines. The uncertainties given in these tables are estimates reflecting both the calibration errors, which are apt to be systematic, and the statistical uncertainties.

The labeling of the l doubled levels follows the suggestion of Brown *et al.* (*10*).

IV. $\nu_4 + 2\nu_7$ COMBINATION BAND

A moderately intense band accompanies each of the ir active fundamentals of C_3O_2, about 50 to 100 cm^{-1} to the high frequency side. This feature has been recognized by Duckett *et al.* (*3*) as a satellite combination band involving $\Delta v_7 = +2$. The Fourier transform spectrum we obtained of the low frequency side of the $\nu_4 + 2\nu_7$ band is given in Fig. 2. The P- and R-branch pattern centered near 1644 cm^{-1} with a bandhead in the P branch is easily recognized and was assigned to the ground state transition. The hot bands are shifted to progressively higher frequencies (opposite to the behavior in the fundamental) and they account for the bulk of the absorption in this region.

The J values in the 1644 subband were assigned in order to obtain agreement with the ground state rotational constants. This led to an inconsistency in the value of the energy of the $\nu_4 + 2\nu^0_7$ state between that determined from this band and from the ν_4 hot band reported in Ref. (*1*). Since the energy of the $2\nu^0_7$ state has been definitely established by Mantz *et al.* (*4*), the only possibility was a misassignment of the J values in the $2\nu^0_7$ hot band of ν_4. This was a distinct possibility in view of the small value of ΔB for that band and the absence of any Q branch. An upward shift of the band origin of the $2\nu^0_7$ hot band of ν_4 by one line position led to complete agreement in the data.

TABLE III. Observed frequencies (vac. cm^{-1}) of the $\nu_4 + 3\nu_7^{3e} \leftarrow 3\nu_7^{3e}$ transitions. The rms error of the fit using the molecular constants in Tables VI and VII is ± 0.0027 cm^{-1} for 29 lines.

J	R(J) OBS.	O-C x 10^3	P(J) OBS.	O-C x 10^3
11			1567.8443	0.6
13			67.5548	2.0
15	1572.0907	-3.4	67.2671	1.9
17	72.4303	-2.6	66.9791	-1.6
19	72.7741	-0.8	66.6961	-3.3
21	73.1148	-5.2	66.4217	0.4
23	73.4678	-0.4	66.1468	0.6
25	73.8196	0.0	65.8748	0.7
27	74.1778	3.9		
29	74.5373	6.0		
31	74.8961	4.5		
33	75.2568	2.1		
35	75.6208	0.2		
37	75.9924	3.1		
41	76.7303	-4.2		
43	77.1094	-1.5		
45	77.4885	-1.2		
47	77.8690	-1.8		
49	78.2546	0.5		
51	78.6361	-3.5		
53	79.0257	-1.4		
55	79.4173	0.8		
57	79.8110	3.3		

The line positions of this $\nu_4 + 2\nu^0_7 \leftarrow 0$ band are reported in Table VIII, along with the molecular constants for the best fit and the difference between the observed and calculated line positions.

The positions of the hot bands for this combination band can be predicted with some exactness—the centers of the two lowest frequency ones are indicated in Fig. 2. However, the Fourier transform spectra could not resolve the individual lines of their overlapping *P* and *R* branches.

TABLE IV. Observed frequencies (vac. cm^{-1}) of the $\nu_4 + 3\nu_7^{3f} \leftarrow 3\nu_7^{3f}$ transitions. The rms error of the fit using the molecular constants in Table VI and VII is ± 0.0030 cm^{-1} for 24 lines.

J	R(J) OBS.	O-C x 10^3	P(J) OBS.	O-C x 10^3
12			1567.6944	-0.9
14	1571.9222	-2.6	67.4081	2.0
16	72.2582	-3.6	67.1193	-0.9
18	72.6012	-0.6	66.8374	-0.2
20	72.9440	-1.0	66.5603	2.1
22	73.2883	-2.8	66.2837	1.8
24	73.6453	5.1	66.0091	0.3
26			65.7361	-2.8
32	75.0716	6.9		
34	75.4314	4.0		
36	75.7959	3.2		
40	76.5279	-2.4		
42	76.8995	-3.0		
44	77.2712	-5.5		
46	77.6508	-2.2		
48	78.0287	-2.4		
50	78.4128	1.8		
52	78.7962	3.7		

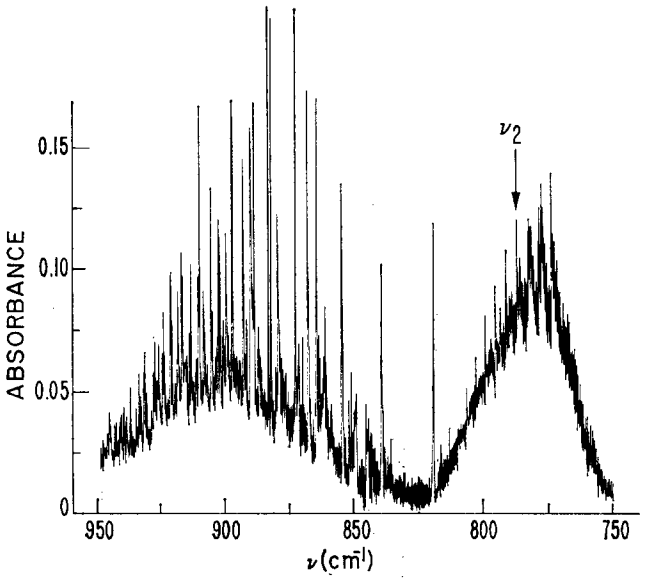

FIG. 3. Fourier transform spectrum of the $\nu_2 \pm \nu_7$ combination bands of C_3O_2. The experimental conditions are the same as those for Fig. 2.

The transitions $\Delta v_4 = +1$, $\Delta v_7 = +4$ and $\Delta v_4 = +1$, $\Delta v_7 = -2$ are observed to be considerably weaker. Although individual rotational lines are seen at this resolution of 0.05 cm^{-1}, they are far too closely spaced and overlapped to be analyzed.

The relative intensities of the various transitions within a given band can be estimated using the Franck–Condon principle in regard to the separation of the high and low frequency vibrations. In the dipole approximation the intensities of the v_4 $1 \leftarrow 0$ transitions are given by (*11*)

$$|\langle v_4 = 1, v'_7, l_7 | M_z | v_4 = 0, v_7, l_7 \rangle|^2.$$

TABLE V. Observed frequencies (vac. cm^{-1}) of the $\nu_4 + 4\nu_7^{\circ} \leftarrow 4\nu_7^{\circ}$ transitions. The rms error of the fit using the molecular constants in Tables VI and VII is ± 0.0014 cm^{-1} for 26 lines.

J	R(J) OBS.	O-C x 10^3	P(J) OBS.	O-C x 10^3
10	1574.6836	2.3		
12	74.9928	1.0		
14	75.3012	-1.2		
16	75.6105	-2.6		
22	76.5440	-1.6		
24	76.8558	-0.8		
26	77.1705	2.8	1568.9734	-0.4
28	77.4791	0.4	68.6658	-2.1
30	77.7926	2.7	68.3620	-0.4
32	78.1015	0.5	68.0563	-0.8
34	78.4129	0.7	67.7534	1.4
36	78.7234	0.1	67.4479	0.8
38	79.0335	-1.0	67.1413	-1.1
40	79.3456	-0.0	66.8375	-0.2
42	79.6581	1.3	66.5314	-1.7
44			66.2280	-0.5
			65.9241	0.3

In the expansion of M_z only the term $(\partial M_z/\partial q_4)_0 . q_4$ is considered important, thus, the intensity factor becomes

$$(\partial M_z/\partial q_4)^2{}_0 |\langle v_4 = 1|q_4|v_4 = 0\rangle|^2 . |\langle v'_7 l_7|v_7 l\rangle|^2. \quad (3)$$

The first two factors can be taken as constants in consideration of the Franck–Condon principle and the extremely low frequency of ν_7. If the ν_7 potential did not change when ν_4 was excited, then the last matrix element in Eq. (3) would vanish unless $v'_7 = v_7$. The rather large strength of the satellite bands thus gives an indication of a large change in the ν_7 potential.

The last matrix element in Eq. (3) is given explicitly as an integral in Eq. (40) of Weber and Ford (*2*), and the wavefunctions needed to evaluate it are determined at the same time the corresponding eigenvalues are found. For the case of the $\nu_4 + 2\nu^0_7 \leftarrow 0$ transition, we predict the intensity to be 7.5% of the ν_4 fundamental. This is in fair agreement with our observed value of 11%, determined from the Fourier transform

TABLE VI. Molecular constants (vac. cm^{-1}) for the ν_7 states of $^{12}C_3{}^{16}O_2$ determined from ν_4 1-0 transitions. Errors are estimated uncertainties. Except for the ground state the uncertainties on H" are at least $1\text{-}2\times10^{-12} cm^{-1}$

State	B"	D"(10^{-8})	H"(10^{-12})
0^c	0.075576 $\pm 2\times10^{-5}$	4.04 $\pm$ 0.4	0.62 $\pm$ 0.1
$\nu_7{}^{1e}$	0.076012 $\pm 3\times10^{-5}$	4.44 $\pm$ 0.71	4.38
$\nu_7{}^{1f}$	0.076450 $\pm 3\times10^{-5}$	5.00 $\pm$ 1.1	4.86
$2\nu_7{}^{2f}$	0.077010 $\pm 3\times10^{-5}$	6.61 $\pm$ 1.0	0.36
$2\nu_7{}^{2e}$	0.076979 $\pm 3\times10^{-5}$	5.76 $\pm$ 1.0	2.6
$2\nu_7{}^{0}$	0.076274 $\pm 3\times10^{-5}$	4.13 $\pm$ 0.9	4.58
$3\nu_7{}^{3e}$	0.077463 $\pm 4\times10^{-5}$	- 2.3 $\pm$ 3.0	0[a]
$3\nu_7{}^{3f}$	0.077510 $\pm 4\times10^{-5}$	3.5 $\pm$ 3.0	0[a]
$3\nu_7{}^{1e}$	0.076616 $\pm 3\times10^{-5}$	0.82 $\pm$ 0.6	- 0.12
$3\nu_7{}^{1f}$	0.077145 $\pm 3\times10^{-5}$	1.57 $\pm$ 0.6	0.02
$4\nu_7{}^{c}$	0.077374 $\pm 3\times10^{-5}$	7.93 $\pm$ 3.5	0.16

[a] D' and H" constrained to zero, all 5 remaining constants fit simultaneously.

TABLE VII. Band origins and molecular constants (vac. cm^{-1}) for the ν_4 1-0 transition of $^{12}C_3{}^{16}O_2$. The estimated errors are approximately 0.003 cm^{-1} on band origins, 5×10^{-6} cm^{-1} on Δ B, $3\text{-}6\times10^{-9}$ cm^{-1} on Δ D, and $0.2\text{-}2\times10^{-12}$ cm^{-1} on Δ H.

Transition	Band Origin	B'-B"(10^{-4})	D'-D"(10^{-8})	H'-H"(10^{-12})
$\nu_4 - 0^o$	1587.390	6.43	1.88	0.17
$\nu_4 + \nu_7{}^{1e} - \nu_7{}^{1e}$	1580.896	4.46	2.0	1.4
$\nu_4 + \nu_7{}^{1f} - \nu_7{}^{1f}$	1580.900	5.35	1.4	-0.01
$\nu_4 + 2\nu_7{}^{2f} - 2\nu_7{}^{2f}$	1575.094	3.96	0.44	-0.3
$\nu_4 + 2\nu_7{}^{2e} - 2\nu_7{}^{2e}$	1575.091	3.95	-0.11	-0.8
$\nu_4 + 2\nu_7{}^{o} - 2\nu_7{}^{o}$	1583.429	-0.074	0.59	0.4
$\nu_4 + 3\nu_7{}^{3e} - 3\nu_7{}^{3e}$	1569.502	4.17	1.08	0[a]
$\nu_4 + 3\nu_7{}^{3f} - 3\nu_7{}^{3f}$	1569.500	4.18	1.21	0[a]
$\nu_4 + 3\nu_7{}^{1e} - 3\nu_7{}^{1e}$	1575.996	1.26	0.19	-0.2
$\nu_4 + 3\nu_7{}^{1f} - 3\nu_7{}^{1f}$	1575.996	1.81	0.28	-0.2
$\nu_4 + 4\nu_7{}^{o} - 4\nu_7{}^{o}$	1572.976	0.25	-0.00	-0.6

[a] H' and H" constrained to zero, all five remaining constants fit simultaneously.

spectra. The various $\Delta v_7 = 0$ hot bands are predicted to have roughly the same intensity, except for Boltzmann factors, which also agrees with our results.

V. $\nu_2 \pm \nu_7$ COMBINATION BANDS

The relatively weak bands centered near 800 and 900 cm^{-1} have been identified by Duckett *et al.* (*3*) as due to $\Delta v_2 = +1$ and $\Delta v_7 = \pm 1$ transitions, with $\Delta l = \pm 1$, and $\Delta J = \pm 1$ or 0. Both bands show a number of sharp peaks, as can be seen in Fig. 3. An arrow indicates the frequency of the ir inactive ν_2 band at 786.1 cm^{-1} (*5*). The "hash" around 825 cm^{-1} is not due to noise, but to individual rotation lines as shown in an expanded plot of that region in Fig. 4. The strong individual peaks above 800 cm^{-1} are the *Q* branches of the combination sum hot bands. The first such peak at 820 cm^{-1} is the ground state transition and some of its *P*- and *R*-branch lines are labeled on Fig. 4. The *P*- and *R*-line positions are listed in Table IX along with the molecular constants that give the best fit to the data and the differences between the observed and calculated line positions. The *B* value of the lower state definitely establishes this to be the ground state transition.

No *P* and *R* branches could be identified in the hot bands due to the overlapping.

The Q branch at 840 cm^{-1} is certainly due to the $\nu_2 + 2\nu^2_7 \leftarrow 1\nu^1_7$ hot band. The shapes of some of the Q branches are quite distorted. In particular the one with a sharp edge at 846.5 cm^{-1} lacks a well-defined peak but has strong absorption extending for nearly 5 cm^{-1} toward lower frequency. This was taken to be the $\nu_2 + 2\nu^0_7 \leftarrow 1\nu^1_7$ Q branch.

Using the method of Ref. (*2*) a potential was determined that gave the best fit to the above Q-branch positions and the B value of the $\nu_2 + \nu^1_7$ state. The energy levels and B values were then calculated from this potential for states through $\nu_2 + 6\nu_7$. First it was noted that the B value calculated for the $\nu_2 + 2\nu^0_7$ state gave a large negative ΔB for the $\nu_2 + 2\nu^0_7 \leftarrow 1\nu^1_7$ Q branch, consistent with its observed width. In addition, the calculated B values were relatively insensitive to changes in the potential constants that produced substantial changes in the energy levels. This led to the expectation that the calculated B values would be reasonably accurate and that the resultant ΔB values for the various transitions would correspond to the observed widths of the Q branches. However, it was impossible to closely fit all of the observed Q-branch positions with the calculated energy levels for the ν_7 and $\nu_7 + \nu_2$ states. Differences of 5 to 10 cm^{-1} occurred for the Q branches involving $v_7 \geq 3$ in the excited state.

During the course of the work, new or more accurate experimental results became available which allowed us to determine a refined ν_7 potential function for both the

TABLE VIII. Observed frequencies (vac. cm^{-1}) of the ground state to $\nu_4 + 2\nu_7^0$ transitions determined from Fourier transform spectra. The lower level constants were constrained to be those from Ref. (*4*). The molecular constants (vac cm^{-1}) and estimated errors are ν_o= 1644.1394 (±0.05), B'-B"= 7.011 (±0.03) × 10^{-4}, D'-D"= -1.896 (±0.07) × 10^{-8}, H'-H" = 7.60 (±1.7) × 10^{-12}, rms error is 0.0065 cm^{-1} for 56 lines.

J	R(J) OBS.	O-C x 10^3	P(J) OBS.	O-C x 10^3
4	1644.9160	-0.1	1643.5405	-2.8
6	45.2324	-4.1	43.2392	-14.5
8	45.5593	-3.4	42.9785	8.7
10	45.8863	-8.1	42.7013	9.8
12	46.2222	-9.7	42.4301	11.1
14	46.5702	-4.9	42.1604	8.1
16	46.9152	-8.9	41.8976	6.2
18	47.2814	2.5	41.6436	7.3
20	47.6445	4.9	41.3920	4.7
22			41.1495	5.2
24			40.9099	2.5
26			40.6764	-0.3
28			40.4519	-0.4
30	49.5443	9.6	40.2335	-0.9
32	49.9255	-7.2	40.0225	-0.6
34			39.8191	0.6
36	50.7345	-14.3	39.6233	2.6
38	51.1601	-7.1	39.4304	0.4
40	51.5903	-2.4	39.2491	1.7
42	52.0257	0.2	39.0719	1.6
44	52.4625	-3.4	38.9001	-1.6
46	52.9115	-2.5	38.7404	-0.5
48			38.5852	-2.9
50	53.8230	-11.4	38.4391	-4.5
52	54.3111	3.8	38.3125	4.9
54	54.7963	7.4	38.1830	2.5
56	55.2829	3.2	38.0609	-1.6
58	55.7741	-5.9	37.9540	0.1
60	56.3044	14.4	37.8606	5.6
62	56.8076	-2.7	37.7769	9.9
64			37.6903	2.1
66	57.8683	-14.8		

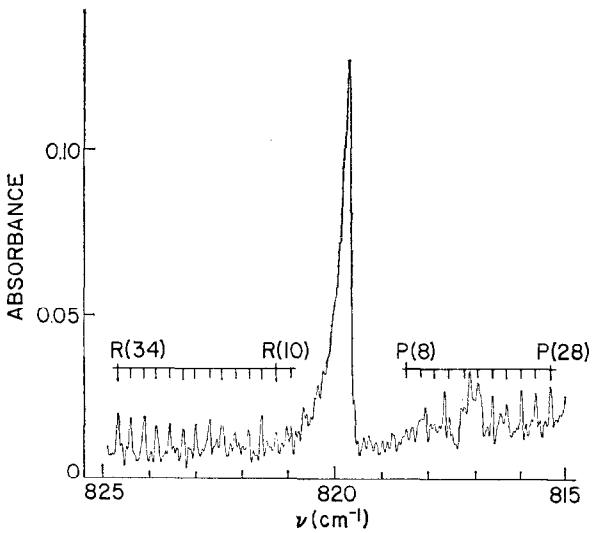

FIG. 4. Fourier transform spectrum showing the unresolved Q branch of the $\nu_2 + \nu^1_7 \leftarrow 0$ transition and the resolved P and R branches. Experimental conditions are the same as those for Fig. 2.

TABLE IX. Observed frequencies (vac. cm^{-1}) of the ground state to $\nu_2 + \nu_7^{1e}$ transitions determined from Fourier transform spectra. The lower level constants were constrained to be those from Ref. (4). The molecular constants (vac. cm^{-1}) with estimated errors are ν_o= 819.6905, B'-B"= -1.817 (±0.04) × 10^{-4}, D'-D" = -1.448 (±0.12) × 10^{-8}, H'-H" = 7.4 (±1.7) × 10^{-13}; rms error is 0.0083 cm^{-1} for 51 lines.

J	R(J) OBS.	O-C x 10^3	P(J) OBS.	O-C x 10^3
8			818.4646	-6.8
10	821.3130	-15.9		
12	821.6386	16.4	817.8573	3.8
14	821.9183	4.2	817.5453	2.7
16	822.2146	10.0		
18	822.4921	-1.8		
20	822.7716	-10.3	816.6033	1.0
22	823.0710	2.3	816.2933	6.8
24	823.3374	-17.0	815.9685	-1.3
26	823.6385	-0.6	815.6571	5.0
28	823.9336	10.8	815.3317	-1.8
30	824.1973	-8.3		
32	824.5008	13.2	814.6752	-10.8
34	824.7769	7.9	814.3770	3.6
36	825.0492	-0.6	814.0443	-8.0
38	825.3376	7.4	813.7205	-10.5
40	825.6132	2.9		
42	825.8957	5.5	813.0896	1.8
44	826.1682	-2.1		
46	826.4578	7.3	812.4449	-0.3
48	826.7314	0.2	812.1161	-8.6
50	827.0059	-6.6	811.8150	10.3
52	827.2980	3.3	811.4943	-1.4
54	827.5716	-8.4		
56	827.8667	4.0	810.8494	-2.1
58			810.5295	-7.3
60	828.4327	-4.7	810.2313	7.2
62	828.7327	4.7	809.9272	13.5
64	829.0313	10.1	809.5966	-19.2
66	829.3215	4.0	809.2913	-9.6

TABLE X. Calculated ν_7 energies and $\bar{B}$ values for the ground state and the ν_2 excited state. The q's for the ℓ=1 states are also listed.

	Ground State		$\nu_2 = 1$	
ν_7^{ℓ}	E	$\bar{B}$	E	$\bar{B}$
0	0	.075563	0	.074779
1^1	18.93	.076310 $q=4.11\times10^{-4}$	33.05	.075567 $q=2.99\times10^{-4}$
2^2	46.30	.076890	70.52	.076155
2^0	60.70	.076220	77.00	.075928
3^3	80.39	.077436	113.78	.076718
3^1	99.19	.077002 $q=5.34\times10^{-4}$	126.05	.076542 $q=4.66\times10^{-4}$
4^4	119.46	.077944	161.04	.077241
4^2	137.44	.077514	171.72	.076989
4^0	144.65	.077274	175.43	.076879
5^5	162.66	.078425	211.70	.077734
5^3	180.71	.078044	222.93	.077488
5^1	195.40	.077866 $q=6.89\times10^{-4}$	234.70	.077451 $q=6.26\times10^{-4}$
6^6	209.44	.078985	265.35	.078204
6^4	227.45	.078543	276.81	.077970
6^2	240.09	.078262	284.60	.077807
6^0	244.55	.078133	287.00	.077734

ground and ν_2 states. From these refined potentials new values for the energy levels and, hence, the Q-branch positions were predicted. The ground state levels were first determined by adjusting the four constants defined in Ref. (*2*) to fit four experimental results: the $2\nu^0_7$ energy (60.70 cm^{-1}) and B value (0.076280), the ground state B value (0.075563) and the ν^1_7 state $\bar{B}$ value (0.076310 cm^{-1}), recently measured by Mantz (*12*). The constants obtained were $\xi = 0.2682$, $B_0 = 0.073771$ cm^{-1}, $V_2 = -1653$ cm^{-1}, and $V_4 = 25\,479$ cm^{-1}, where ξ is the ratio of the bending mode reduced mass to the moment of inertia, both measured in the linear position; B_0 is the linear position rotational constant; and V_2 and V_4 are the quadratic and quartic coefficients in the potential function $V(\alpha) = V_2 \sin^2\alpha + V_4 \sin^4\alpha$, where 2α is the angular deviation of the molecule from linearity. These yield a 26.8 cm^{-1} potential barrier and a minimum at $\alpha = 10.38°$. The reduced mass for the bending mode is found to be $\mu = 61.29$ amu-Å^2, which is somewhat greater than that in Ref. (*3*).

For the potential in the $v_2 = 1$ state, we kept $\xi = 0.2682$ and fit three experimental numbers: $(2\nu^0_7 + \nu_2) - \nu_2 = 77.0$ cm^{-1}, $(2\nu^0_7 + \nu_2) - (2\nu^2_7 + \nu_2) = 6.5$ cm^{-1}, and $B(2\nu^0_7 + \nu_2) = 0.075928$ cm^{-1}. The first of these numbers was determined from a preliminary high resolution Raman spectrum by Brodersen (*13*) and the last two from diode laser spectra of the $\nu_2 + 2\nu^2_7 \leftarrow \nu^1_7$ and $\nu_2 + 2\nu^0_7 \leftarrow \nu^1_7$ Q branches (*14*). The

TABLE XI. Q branches of the hot bands of $\nu_2+\nu_7$ of C_3O_2. The position is that observed for the leading edge of a shaded Q branch. The assignment is for the ν_7 states. The calculated Q-branch positions and ΔB's are obtained using the data in Table X with $\nu_2 = 787.8$ cm^{-1}. Values in parentheses are uncertain.

Transition	Obs.(cm^{-1})	Obs.-Cal.	Predicted ΔB(10^{-4}cm^{-1}
$1^1 \leftarrow 0^0$	819.7	-1.2	+1.5
$2^2 \leftarrow 1^1$	840.0	0.6	-3.6 & +1.5
$2^0 \leftarrow 1^1$	846.5	0.6	-5.9
$3^1 \leftarrow 2^0$	849.8	-3.3	+5.0
$3^3 \leftarrow 2^2$	855.8	+0.5	-1.7
$3^1 \leftarrow 2^2$	865.4	-2.1	-5.9 & -1.2
$4^2 \leftarrow 3^1$	862.0	+1.7	-2.5 & +2.5
$4^0 \leftarrow 3^1$	(864.8)	+0.7	-3.9
$4^4 \leftarrow 3^3$	869.0	+0.6	-2.0
$4^2 \leftarrow 3^3$	(880)[a]	±1	-4.5
$5^1 \leftarrow 4^0$	(872.3 or 877.4)	-5.5 or -0.5	+4.9
$5^3 \leftarrow 4^2$	873.7	+0.4	-0.3
$5^1 \leftarrow 4^2$	883.0 or 884.4	-2.0 or -0.7	-3.9 & +2.5
$5^5 \leftarrow 4^4$	880.8[a]	+0.7	-2.1
$5^3 \leftarrow 4^4$	891.3	0	-4.6
$6^0 \leftarrow 5^1$	(880)[a]	±1	-4.8
$6^2 \leftarrow 5^1$	(880)[a]	~2-3	-4.0 & +2.9
$6^4 \leftarrow 5^3$	884.4 or 883.0	+0.6 or -0.8	-0.7
$6^2 \leftarrow 5^3$	894.2 or 891.6	+2.6 or 0	-2.4
$6^6 \leftarrow 5^5$	889.8	-0.7	-2.2
$6^4 \leftarrow 5^5$	900.9	-1.1	-4.6

[a]Several overlapping Q branches span the 879.5 – 880.8 region.

resulting potential constants were $B_0 = 0.073697$ cm^{-1}, $V_2 = -342.5$ cm^{-1}, and $V_4 = 23\,720$ cm^{-1}, which lead to a 1.24 cm^{-1} barrier and a minimum at 4.9°. A summary of the calculated energy levels and rotational constants for the ν_7 levels in the ground and $v_2 = 1$ states is given in Table X.

The Q-branch assignments decided upon are listed in Table XI. For the purpose of determining calculated Q-branch positions, we used the results in Table X with $\nu_2 = 787.8$ cm^{-1}, rather than 786.1 cm^{-1} as given by Carreira *et al.* (*5*), on the basis that it gave the best fit to the three lowest Q branches. This value is within a few tenths of a cm^{-1} of the value for ν_2 indicated on Brodersen's preliminary spectrum. Great reliance was made on the predicted ΔB values for each transition, which are also listed. Expanded plots of the spectrum were used, and the position of a Q branch is that determined for its leading edge when it was appreciably shaded as a consequence of a large ΔB value. The Q-branch frequencies in parentheses in the table are uncertain for one or more

reasons such as a sizeable difference in frequency from that predicted, abnormal intensity, a width not commensurate with the predicted ΔB value, etc. In other cases there was no reason to choose between two possible assignments. The fit to the observed spectrum is mostly better than 1 cm^{-1} except for transitions to $l = 1$ states of $\nu_2 + \nu_7$ for which differences of several cm^{-1} occur. Our assignments agree with those made by Duckett *et al.* (*3*) for states with l equal to v_7 except for the $6^6 \leftarrow 5^5$ case.

The difference band ($\Delta v_2 = +1$, $\Delta v_7 = -1$, $\Delta l = \pm 1$), which appears in Fig. 3 in the region from 750 to 800 cm^{-1} also shows a number of peaks that give the appearance of Q branches just as for the sum band. However, the ΔB values predicted from the previous data for these transitions are all large and negative. As a consequence, the Q branches would be quite spread out with no appreciable peaks, and hence would be difficult to recognize. But the large ΔB values can lead to the development of bandheads in the R branches which would appear as fairly sharp peaks with sharp high frequency edges, as was suggested by Carreira *et al.* (*5*) in the case of the ν_7 band. To check this assertion, we calculated the line positions for the first few difference bands using either the molecular constants given in Table X (including the D terms which are not listed) or, where available, the constants determined from other experiments (*1*, *4*, *12*, *14*).

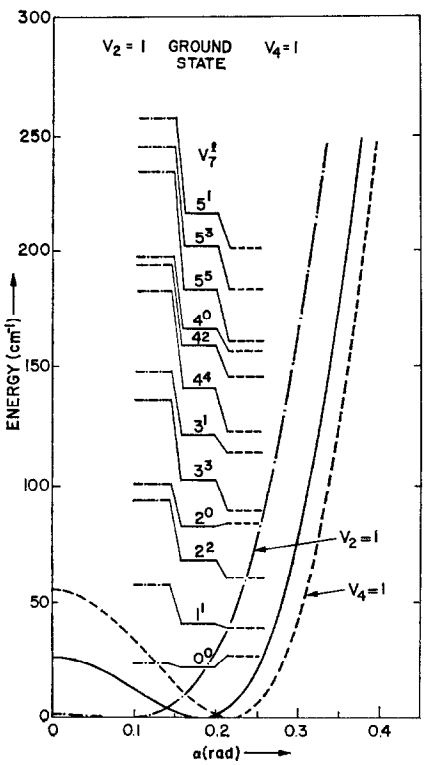

FIG. 5. Potential curves and calculated energy levels of the ν_7 vibration. Solid lines for the ground state, dashed lines with ν_4 (1587.4 cm^{-1}) excited, and the broken lines with ν_2 (786.1 cm^{-1}) excited. Differences between observed and calculated energy levels are too small to show on this scale. The potentials are arbitrarily set to zero at their minima.

For the $\nu_2 \leftarrow \nu^1{}_7$ transition with its center expected to be at 768.9 cm^{-1}, a bandhead is predicted for the $R(57)$ line at 773.2. There is no indication of a Q branch in the absorption spectrum around 769 cm^{-1}. We would identify as the bandhead the lowest frequency peak at 773.8 cm^{-1}. It is shaded to lower frequencies as would be expected. Althouth it lies 0.6 cm^{-1} higher than expected there is a large uncertainty in predicting this bandhead position since we rely entirely on the model predictions for the upper state constants. The $\nu_2 + \nu^1{}_7 \leftarrow 2\nu^0{}_7$ transition should be centered at 760.1 cm^{-1} and no bandhead is predicted. Again there is no indication of the presence of a Q branch in this region. The band center for the $\nu_2 + \nu^1{}_7 \leftarrow 2\nu^2{}_7$ transitions should be near 774.5 cm^{-1} and bandheads are predicted at the $R(50)$ line at 778.3 cm^{-1} (for even J lower states) and at the $R(59)$ line at 779.2 cm^{-1} (for odd J lower states). These bandheads are predicted using measured molecular constants for both the lower and upper states and consequently are expected to be quite accurate. There are peaks at 777.2, 778.0, and 779.1 cm^{-1} in this region from which we would select the highest two as the bandheads. Although the peak at 773.8 cm^{-1} that we have interpreted as the bandhead of the $\nu_2 \leftarrow \nu^1{}_7$ transition falls near the expected position of the Q branch for $\nu_2 + \nu^1{}_7 \leftarrow 2\nu^2{}_7$, its width is far too narrow for it to be considered as that Q branch. Similarly we would label the other peaks at higher frequencies as bandheads of higher ν_7 states, and we feel that the interpretation of the peaks of this band offered by Duckett *et al.* (*3*) is in error.

VI. DISCUSSION

The predictions from the model for C_3O_2 used by Weber and Ford (*2*) based on a potential having a negative quadratic term and a positive quartic term are in good agreement with the measurements of the hot bands of ν_4 that extended up to the $v_7 = 4$ state. The energy levels of both the ν_7 states and the $\nu_7 + \nu_4$ states are generally within a few tenths of a cm^{-1} of those deduced from the observations. The rotational constant B is fit to about 0.1% accuracy for these levels, and the D value usually within a factor of 2 or 3. The potential functions and the calculated ν_7 energy levels are shown in Fig. 5, the solid lines for the ground state and the dashed lines for $v_4 = 1$. On this scale the difference between the observed and calculated energies is too small to be seen.

The data derived for ν_7 with ν_2 excited to the $v_2 = 1$ state cannot be fit as well by the model. The difference between observed and calculated values for most energy levels is less than 1 cm^{-1}, but for the $l = 1$ states it becomes 2 or 3 cm^{-1}. These differences would barely show in Fig. 5 where the potential chosen and energy levels are plotted with the dash–dot lines. No doubt some of the difficulty arises because of the quite small potential maximum on axis. The coefficient of the negative quadratic term is correspondingly small and the positive quartic term dominates the solutions. But in the case of a small potential hump, one would expect a more nearly harmonic behavior of the upper levels or a positive quadratic term in the potential.

It should be noted that transitions involving $\Delta v_7 = 1$ and $\Delta l = \pm 1$ (as for the far infrared ν_7 band or the $\nu_2 + \nu_7$ band) are a more severe test of the model than those having Δv_7 and Δl equal to zero (as for the hot band shifts in ν_4). In the first case the absolute value of the l splitting in adjacent states is involved, but in the latter case only the change in a particular l level in going from the state $v_4 = 0$ to $v_4 = 1$ matters. For this reason the ν_7 energy levels calculated from the model for the ground state or the $v_4 = 1$ state may not be as accurate as would be concluded from the agreement with the hot band shift data.

Further information on the ν_7 energy levels could be obtained from the far infrared absorption only with greatly improved resolution, but there are existing FTS instruments of that capability. There is, however, the difficulty that transitions between the upper states all tend to fall in the 40 to 70 cm^{-1} region and also have large ΔB values. Consequently the Q branches would be difficult to identify and the P and R branches would be too overlapped to separate. On the other hand, the Q branches in the $\nu_7 + \nu_2$ combination band are well separated and further diode laser measurements of them should be both feasible and fruitful. Further measurements of hot band shifts in the ν_4 band from diode laser spectra would be exceedingly tedious since the individual P and R lines become quite weak for $v_7 > 4$, and the series of the many hot bands are all intermingled. On the other hand, in the near infrared band at 3200 cm^{-1} originally studied by Lafferty *et al.* (*15*) and more recently by Mantz *et al.* (*4*) the hot bands are appreciably displaced from each other, so that accurate B values of the lower state levels could be obtained. It would also be interesting to study the hot bands in the ν_6 bending vibration at 550 cm^{-1} to see the effect of that type of vibration on the ν_7 states. The ΔB values for this case are estimated to be small, so that the Q branches of the hot bands due to ν_7 should be fairly sharp.

It also appears that there may be anomalies in the relative intensities of the ν_l hot bands in the Raman spectrum of ν_2. In particular, the ν_2 fundamental seems weaker than some of the $l = 0$ hot bands. The overlap integral method used here to estimate the intensity of the $\nu_4 + 2\nu_7$ combination band should be applicable to that situation also.

ACKNOWLEDGMENTS

We thank I. M. Mills for sending us a copy of Ref. (*3*) prior to publication, A. W. Mantz for communicating his unpublished results, and H. Niki, L. P. Breitenbach, and N. Savage for help in obtaining the FTS spectra. We are particularly grateful to S. Brodersen for sending us a copy of his preliminary Raman spectrum of the ν_2 region, which aided considerably in our Q-branch assignments.

RECEIVED: February 2, 1977

REFERENCES

1. W. H. WEBER, P. D. MAKER, AND C. W. PETERS, *J. Chem. Phys.* **64**, 2149 (1976).
2. W. H. WEBER AND G. W. FORD, *J. Mol. Spectrosc.* **63**, 445 (1976).
3. J. A. DUCKETT, I. M. MILLS, AND A. G. ROBIETTE, *J. Mol. Spectrosc.* **63**, 249 (1976).
4. A. W. MANTZ, P. CONNES, G. GUELACHVILI, AND C. AMIOT, *J. Mol. Spectrosc.* **54**, 43 (1975).
5. L. A. CARREIRA, R. O. CARTER, J. R. DURIG, R. C. LORD, AND C. C. MILIONIS, *J. Chem. Phys.* **59**, 1028 (1973).
6. F. A. MILLER AND W. G. FATELEY, *Spectrochim. Acta* **20**, 253 (1964).
7. F. BARTOLI, R. ALLEN, L. ESTEROWITZ, AND M. KRUER, *J. Appl. Phys.* **45**, 2150 (1974).
8. G. D. BERGLAND, *Comm. ACM* **11**, 703 (1968).
9. R. B. SANDERSON AND E. E. BELL, *Appl. Opt.* **12**, 266 (1973).
10. J. M. BROWN, J. T. HOUGEN, K.-P. HUBER, J. W. C. JOHNS, I. KOPP, H. LEFEBVRE-BRION, A. J. MERER, D. A. RAMSAY, J. ROSTAS, AND R. N. ZARE, *J. Mol. Spectrosc.* **55**, 500 (1975).
11. G. HERZBERG, "Spectra of Diatomic Molecules," 2nd ec., p. 199, Van Nostrand, New York, 1950; "Infrared and Raman Spectra," p. 252, Van Nostrand, New York, 1945.
12. A. W. MANTZ, private communication.
13. S. BRODERSEN, private communication.
14. W. H. WEBER, J. P. ALDRIDGE, H. FLICKER, N. G. NERESON, H. FILIP, AND M. J. REISFELD, *J. Mol. Spectrosc.* **65**, 474 (1977).
15. W. J. LAFFERTY, A. G. MAKI, AND E. K. PLYLER, *J. Chem. Phys.* **40**, 224 (1964).